Affect of the lanthanide ionic radius on the Raman spectroscopy of lanthanide agardite minerals

Ray L. Frost[1•], Kristy L. Erickson[1], Matt L Weier[1], Adam R. McKinnon[2], Peter A. Williams[2] and Peter Leverett[2]

[1]Inorganic Materials Research Program, School of Physical and Chemical Sciences, Queensland University of Technology, GPO Box 2434, Brisbane Queensland 4001, Australia.

[2]School of Science, University of Western Sydney, Locked Bag 1797, Penrith South DC NSW 1797, Australia.

Published as:
R.L. Frost & K.L. Erickson, M.L. Weier, A.R. McKinnon, P.A. Williams, and P. Leverett, Effect of the lanthanide ionic radius on the raman spectroscopy of lanthanide agardite minerals. *Journal of Raman Spectroscopy*, 2004. 35(11): p. 961-966.

Abstract:

Raman microscopy has been used to study the Raman spectra of a series of rare earth element agardites $ACu_6(AsO_4)_3(OH)_6.3H_2O$ where A = lanthanide^{3+}. These minerals have a porous framework similar to that of zeolites with a structure based upon $(A^{3+})_{1-x}(A^{2+})_xCu_6(OH)_6(AsO_4)_{3-x}(AsO_3OH)_x$. Two sets of AsO stretching vibrations were found and assigned to the vibrational modes of AsO_4 and $HAsO_4$ units. The position of selected bands was found to be sensitive to the lanthanide ionic radius. Raman spectra of the low wavenumber region are complex. Bending modes of the AsO_4 and $HAsO_4$ units were found to be sensitive to the ionic radius of the lanthanide ion. Linear relationships between positions of the Raman bands were derived, with correlation coefficients > 0.90.

Key words- agardite, goudeyite, mixite, petersite, Raman spectroscopy

INTRODUCTION

Agardite is a member of the mixite group, $ACu_6(AsO_4)_3(OH)_6.3H_2O$ for the fully hydrated formula, with (A = lanthanide^{3+}). Mixite (A = Bi), goudeyite (A = Al), zalesiite (A = Ca, with protonation of the lattice for charge compensation) and petersite-(Y), the phosphate analogue of agardite-(Y) are recognized isomorphous species in the group. Of the many possible rare earth congeners constituting the agardite group, only agardite-(Y) and agardite-(La) are recognized as distinct species by the IMA. [1] Others have been reported in the literature [2-7] but their species status remains unresolved. It should be noted that formulae given above refer to ideal, end-member compositions; extensive solid solution in the A site and involving P for As is

• Author to whom correspondence should be addressed (r.frost@qut.edu.au)

known for naturally occurring material. Water in the lattice is for the most part thought to be zeolitic in nature, as evidenced by single-crystal X-ray structure determinations. [8-10] The crystal structures of natural mixite and agardite compounds reveal a microporous framework structure [4,8] with a framework similar to that of zeolites. [10] Dietrich et al. [11] originally proposed that the water in agardite was zeolitic. As such these minerals may have potential for catalytic applications.

The mixite group consists of secondary minerals formed through crystallisation from aqueous solution. The conditions under which this crystallisation takes place, particularly relating to anion and cation concentrations, pH, temperature and kinetics of crystallisation, determines the particular mineral that is formed. Recently, Raman spectroscopy has been used to gain an understanding of many properties of secondary minerals. [12-18] In particular, Raman spectroscopy has been used to determine paragenetic relationships between many closely related phases. In this paper we report the Raman spectroscopic analysis of a set of synthetic lanthanide agardite minerals and a relationship involving spectroscopic parameters and the ionic radii of the lanthanide (REE) elements. (REE=rare earth element)

Synthesis of lanthanide agardites

Pure end-members of the agardite group were synthesized in the following way. To 30 cm^3 of water in a 250 cm^3 Teflon-lined acid digestion bomb was added with stirring 6.0 mmol of $Cu(NO_3)_2.2.5H_2O$, 3.0 mmol of $Na_2HAsO_4.7H_2O$, and 1.0 mmol of $Y(NO_3)_3.6H_2O$. The pH of the mixture was adjusted to 6.6 by dropwise addition of 1.0 M aqueous NaOH. The bomb was sealed and the mixture heated at 180^{o}C for 48 hours, then cooled to room temperature. The product, agardite-(Y), was filtered off, washed with water, then acetone and sucked dry at the pump (yield > 95%). Powder X-ray diffraction using a Phillips PW1825 X-ray diffractometer with Mo Kα radiation showed that a single crystalline phase was present. Separate pure samples of agardite-(La), -(Ce), -(Pr), -(Nd), -(Sm) and -(Eu) were prepared in identical fashion with similar yields by substituting the appropriate hydrated REE nitrate for $Y(NO_3)_3.6H_2O$. The minerals were checked for phase integrity using powder X-ray diffraction and for chemical composition using an electron probe.

Raman microprobe spectroscopy

The crystals of the agardites were placed and oriented on a polished metal surface on the stage of an Olympus BHSM microscope, equipped with 10x and 50x objectives. The microscope is part of a Renishaw 1000 Raman microscope system, which also includes a monochromator, a notch filter system and a thermo-electrically cooled Charge Coupled Device (CCD) detector. Raman spectra were excited by a HeNe laser (633 nm) at a resolution of 2 cm^{-1} in the range between 100 and 4000 cm^{-1}. Repeated acquisition using the highest magnification was accumulated to improve the signal to noise ratio. Spectra were calibrated using the 520.5 cm^{-1} line of a silicon wafer. In order to ensure that the correct spectra are obtained, the incident excitation radiation was scrambled. The crystals were oriented to provide maximum intensity. All crystal orientations were used to obtain the spectra. Power at the sample was measured as 1 mW.

The Galactic software package GRAMS was used for data analysis. Band component analysis was undertaken using the Jandel 'Peakfit' software package, which enabled the type of fitting function to be selected and allows specific parameters to be fixed or varied accordingly. Band fitting was carried out using a Gauss-Lorentz cross-product function with the minimum number of component bands used for the fitting process. The Gauss-Lorentz ratio was maintained at values greater than 0.7 and fitting was undertaken until reproducible results were obtained with squared regression coefficient of R^2 greater than 0.995.

RESULTS AND DISCUSSION

Agardite-(Ce), for example, is the mineral ($CeCu_6(AsO_4)_3(OH)_6.3H_2O$). Three different vibrating units will contribute to the overall spectral profile, namely the OH units, the water molecules and the AsO_4 groups. The first two vibrating species will contribute to the high wavenumber region whilst the AsO_4 units will show Raman bands below 1200 cm^{-1}. [19] It has been shown that the water can be reversibly lost and the number of water molecules per formula unit can vary up to 3. Raman spectra of lanthanide agardites are shown in Figures 1-3. Figure 1 displays the AsO_4 stretching region, Figure 2 the 350 to 550 cm^{-1} wavenumber range and Figure 3 the 100 to 350 cm^{-1} range. Results of the Raman spectroscopic analyses are reported in Table 1. The Table reports two types of data, namely (a) Raman bands which are sensitive to the REE and (b) bands which do not appear to be affected by the REE (the first type of bands is shown in italics). According to Mereiter and Preisinger (1986) mixites have a microporous framework structure based upon $(M^{3+})_{1-x}(M^{2+})_xCu_6(OH)_6(AsO_4)_{3-x}(AsO_3OH)_x$. [20], with vacancies in the A site or substitution by divalent cations being compensated by protonation of the lattice. On the spectroscopic time scale, exchange of protons between water molecules and arsenate ions is also likely. According to this formulation two types of units involving As are found, namely AsO_4 and $HAsO_4$. Thus two sets of bands involving AsO stretching modes would be expected.

Vibrational spectroscopy has been used to study the coordination chemistry of $(AsO_4)3^-$ ions for some considerable time. [19,21-25] Vansant et al. showed the frequencies of the $(AsO_4)^{3-}$ units of Td symmetry as 818 (A_1), 786 (F-stretching), 405 (F-bending) and 350 cm^{-1} (E). [23] Vibrational spectroscopic studies have shown that the symmetry of the $(AsO_4)^{3-}$ polyhedron are strongly distorted and the $(AsO_4)^{3-}$ vibrations are strongly influenced by the protonation, cation presence and water coordination. [22-25] The symmetric stretching vibration of the arsenate anion in aqueous systems (ν_1) is observed at 810 cm^{-1} and coincides with the position of the antisymmetric stretching mode (ν_3). [19] The symmetric bending mode (ν_2) is observed at 342 cm^{-1} and the (ν_4) bending modes at 398 cm^{-1}. [14,19,26-28] Of all the tetrahedral oxyanions, the positions of the arsenate vibrations occur at lower wavenumbers than any of the other naturally occurring mineral oxyanions.

Two Raman bands are observed in the region 885 to 915 cm^{-1} and in the 867 to 870 cm^{-1} region. These are assigned to the AsO stretching vibrations of $(HAsO_4)^{2-}$ and $(H_2AsO_4)^-$ units. [22,23] According to Myeni et al. (see Myeni table 3) the band at around 915 cm^{-1} corresponds to the antisymmetric stretching vibration of protonated

$(AsO_4)^{3-}$ units and the band at around 870 cm^{-1} to the symmetric stretching vibration of the protonated $(AsO_4)^{3-}$ units. [24,25] The position of the bands indicate a C_{2v} symmetry of the $(H_2AsO_4)^-$ anion. The position of these bands is influenced by the ionic radius of the REE (Table 1). The reason why there is a dependence of the Raman band position and the lanthanide ionic radius is that these bands are due to the vibrations of protonated $(AsO_4)^{3-}$ units. The values of the band positions change because the bond length of the AsO and HAsO distances change with the cation. In contrast two bands are found at around 803 and 833 cm^{-1}. These are assigned to the stretching vibrations of uncomplexed $(AsO_4)^{3-}$ units. The bands correspond to the antisymmetric (803 cm^{-1}) and symmetric (833 cm^{-1}) stretching vibrations of $(AsO_4)^{3-}$ units of T_d symmetry. [24,25] These bands were not sensitive to the ionic radius of the REE. The AsO bond lengths in $(AsO_4)^{3-}$ units are not influenced by protonation or cationic complexation.

A number of bands are observed in the 350 to 550 cm^{-1} region (Figure 2). A band is observed at around 539 cm^{-1} which is cation sensitive. One possible assignment is that the band is the ν_4 bending mode of $(HAsO_4)^-$ units. Such a band position was not observed in the work of Vansant et al. [22,23] and was not reported as was any of the bending modes in the work of Myeni et al. [24,25] The reason why the band is sensitive to the cation is attributed to the changes in bond distances of the REE-O-As and REE-OH-AsO distances. Theoretical studies have shown such bond distances are dependent upon the type of arsenate unit in the structure. [24,25] (see for example Table 2 in the Myeni reference). Such bond distances are cation sensitive for example the As-O bond distance is 1.62 Å for $Al\text{-}O_2\text{-}AsO_2(H_2O)_4$, 1.65 Å for $Mg\text{-}O_2\text{-}AsO_2(H_2O)_4$, 1.66 Å for $CdO_2\text{-}AsO_2(H_2O)_4$ and 1.64Å for $Cd\text{-}O_2\text{-}AsO_2(H_2O)_4$. Such cationic sensitivity is expected to be translated to the bending modes of the $(HAsO_4)^-$ units. Vansant et al showed the potential energy distributions for $(AsO_4)^{3-}$, $(HAsO_4)^{2-}$ and $(H_2AsO_4)^-$ units. [22] These distributions were then used to calculate the attribution of the vibrational modes. [22] A low intensity band is observed at around 492 cm^{-1} which is not cation sensitive. Another intense and REE sensitive band is observed at 486 cm^{-1} and is assigned to the ν_4 antisymmetric bending mode of AsO_4 units. An additional band is observed around 468 cm^{-1} which is not affected by the presence of the REE. Three bands are observed at around 434, 400 and 324 cm^{-1} and are of similar intensities. These are assigned to the ν_2 bending modes of the $HAsO_4$ (434 and 400 cm^{-1}) and the AsO_4 groups (324 cm^{-1}). Bands are found in the 167 to 294 cm^{-1} region which are not REE sensitive. The attribution of these bands is not known. However a REE sensitive band is found at around 142 cm^{-1} assigned to a REE-O stretching vibration. Such a band is expected to be sensitive to the lanthanide cationic radius.

The relationships between the position of the Raman bands listed above and which proved to be sensitive to the presence of the lanthanide, and ionic radius are shown in Figures 4 to 14. Each of these Figures represents the variation of the position of a particular band with lanthanide ionic radius. Figure 4 shows the variation of the ~890 cm^{-1} band attributed to the antisymmetric stretching vibration of the $HAsO_4$ units with ionic radius. The correlation was determined as $R^2 = 0.9396$ and the relationship between band position of the 890 cm^{-1} band and ionic radius is $y = -3.2371x + 1266.8$. A similar function is observed for the ~869 cm^{-1} band (Figure 5) assigned to the antisymmetric stretching vibration of the AsO_4 units. Now the linear function between wavenumber and ionic radius is represented by $y = -0.2261x$

+ 894.38 with R^2 = 0.9039. Thus for both these bands the correlation between the positions of the antisymmetric stretching bands and the lanthanide ionic radius is excellent. The correlation is not good for all bands. For example the band at ~805 cm^{-1} is not as good (Figure 6). The linear relationship is good except from Pr and La. It is proposed that this band is not influenced by the ionic radius.

Such correlation is not as good for the band at around 505 cm^{-1} as shown in Figure 7. The value of R^2 is now 0.4539 and the relationship is given by y = -1.1184x + 626.15. An excellent correlation is found for the band at around 480 cm^{-1} (Figure 8). The R^2 is 0.9865 with the relationship given by y= -0.8537x + 576.88. The relationship is good for the bands at around 430 cm^{-1} (Figure 9) and ~ 396 cm^{-1} (Figure 10). Here the correlation coefficients are 0.9699 and 0.9841. Figure 9 shows the variation for the ~ 395 cm^{-1} band and Figure 10 for the ~320 cm^{-1} band. Figure 11 shows the variation for the ~321 cm^{-1} band; here the relationship is y = -0.4741x + 375.27 with R^2 = 0.9567. Figure 12 shows the relationship for the band assigned to the REE-O stretching vibration. The correlation is reasonably good with R^2 = 0.8634. Similar results are found for the ~237 and ~175 cm^{-1} band.

CONCLUSIONS

A suite of lanthanide agardites of formula $ACu_6(AsO_4)_3(OH)_6.3H_2O$ where A is $lanthanide^{3+}$ has been examined. Two sets of AsO stretching vibrations were found and assigned to the vibrational modes of AsO_4 and $HAsO_4$ units. Both the stretching and bending modes of the $HAsO_4$ units were found to be sensitive to the ionic radius of the trivalent lanthanide ion. Whereas the modes of the AsO_4 units were found to be not effected by the change in the ionic radius of the REE^{3+}. The relationship between the position of the Raman bands and the ionic radius was found to be linear with in many cases the R^2 correlation coefficients > 0.95. Not all band positions were a linear function of the ionic radius.

Acknowledgments

The financial and infrastructure support of the Queensland University of Technology Inorganic Materials Research Program of the School of Physical and Chemical Sciences is gratefully acknowledged. The Australian Research Council (ARC) is thanked for funding.

References

1. Anthony, JW, Bideaux, RA, Bladh, KW, Nichols, MC. *Handbook of mineralogy Vol.V. Borates, Carbonates, Sulphates. - Mineral Data Publishing, Tucson, Arizona* 2003.
2. Olmi, F, Sabelli, C, Brizzi, G. *Mineralogical Record* 1988**; 19**: 305.
3. Braithwaite, RSW, Knight, JR. *Mineralogical Magazine* 1990**; 54**: 129.
4. Hess, H. *Neues Jahrbuch fuer Mineralogie, Monatshefte* 1983: 385.
5. Dunin-Barkovskaya, EA. *Miner. Uzb.* 1976**; 3**: 25.
6. Krause, W, Bernhardt, HJ, Blass, G, Effenberger, H, Graf, HW. *Neues Jahrbuch fuer Mineralogie, Monatshefte* 1997: 271.
7. Walenta, K. *Neues Jahrbuch fuer Mineralogie, Monatshefte* 1960: 223.
8. Aruga, A, Nakai, I. *Acta Crystallographica, Section C: Crystal Structure Communications* 1985**; C41**: 161.
9. Bayliss, P, Lawrence, LJ, Watson, D. *Australian Journal of Science* 1966**; 29**: 145.
10. Miletich, R, Zemann, J, Nowak, M. *Physics and Chemistry of Minerals* 1997**; 24**: 411.
11. Dietrich, JE, Orliac, M, Permingeat, F. *Bulletin de la Societe Francaise de Mineralogie et de Cristallographie* 1969**; 92**: 420.
12. Frost, RL, Crane, M, Williams, PA, Kloprogge, JT. *Journal of Raman Spectroscopy* 2003**; 34**: 214.
13. Frost, RL. *Spectrochimica Acta, Part A: Molecular and Biomolecular Spectroscopy* 2003**; 59A**: 1195.
14. Frost, RL, Kloprogge, JT. *Spectrochimica Acta, Part A: Molecular and Biomolecular Spectroscopy* 2003**; 59A**: 2797.
15. Frost, RL, Duong, L, Martens, W. *Neues Jahrbuch fuer Mineralogie, Monatshefte* 2003: 223.
16. Frost, RL, Williams, PA, Kloprogge, JT, Martens, W. *Neues Jahrbuch fuer Mineralogie, Monatshefte* 2003: 433.
17. Martens, W, Frost, RL, Kloprogge, JT, Williams, PA. *Journal of Raman Spectroscopy* 2003**; 34**: 145.
18. Martens, WN, Frost, RL, Williams, PA. *Neues Jahrbuch fuer Mineralogie, Monatshefte* 2003: 337.
19. Ross, SD *Inorganic Infrared and Raman Spectra (European Chemistry Series)*, 1972.
20. Mereiter, K, Preisinger, A. *Anzeiger der Osterreichischen Akademie der Wissenschaften, math.-natuwiss. Klasse* 1986**; 123**: 79.
21. Siebert, H. *Z. anorg. u. allgem. Chem.* 1954**; 275**: 225.
22. Vansant, FK, Van der Veken, BJ. *Journal of Molecular Structure* 1973**; 15**: 439.
23. Vansant, FK, Van der Veken, BJ, Desseyn, HO. *Journal of Molecular Structure* 1973**; 15**: 425.
24. Myneni, SCB, Traina, SJ, Waychunas, GA, Logan, TJ. *Geochimica et Cosmochimica Acta* 1998**; 62**: 3499.
25. Myneni, SCB, Traina, SJ, Waychunas, GA, Logan, TJ. *Geochimica et Cosmochimica Acta* 1998**; 62**: 3285.

26. Martens, W, Frost, RL, Kloprogge, JT. *Journal of Raman Spectroscopy* 2003**;** **34**: 90.
27. Martens, W, Frost, RL, Williams, PA. *Journal of Raman Spectroscopy* 2003**;** **34**: 104.
28. Martens, WN, Frost, RL, Kloprogge, JT, Williams, PA. *American Mineralogist* 2003**;** **88**: 501.

List of Figures

List of Tables

Table 1 Results of the Raman spectroscopic analysis of synthetic rare earth agardites **.

Band	Y Band Centre (cm^{-1}) / Intensity (%)	Eu Band Centre (cm^{-1}) / Intensity (%)	Sm Band Centre (cm^{-1}) / Intensity (%)	Pr Band Centre (cm^{-1}) / Intensity (%)	Ce Band Centre (cm^{-1}) / Intensity (%)	La Band Centre (cm^{-1}) / Intensity (%)
1	*915 / 4.28*	*907 / 3.03*	*902 / 4.34*	*885 / 7.03*	*885 / 9.64*	*888 / 11.48*
2	*870 / 36.11*	*870 / 38.61*	*868 / 38.41*	*868 / 33.72*	*868 / 34.62*	*867 / 31.56*
3	833 / 13.10	833 / 11.54	832 / 13.21	833 / 9.78	834 / 13.51	832 / 12.34
4	798 / 2.95	803 / 4.88	803 / 2.77	810 / 4.33	809 / 5.81	803 / 4.75
5	557 / 0.39		574 / 1.50			
6	*539 / 1.14*	*534 / 2.27*	*532 / 2.53*	*528 / 3.14*	*527 / 1.66*	*524 / 2.50*
7	514 / 0.28	492 / 3.81	493 / 3.83	500 / 0.99	493 / 2.51	491 / 1.30
8	*486 / 17.17*	*481 / 11.53*	*479 / 12.04*	*476 / 12.30*	*475 / 12.07*	*473 / 9.21*
9	468 / 0.32	465 / 1.17	464 / 0.94	473 / 7.40	461 / 1.61	470 / 4.75
10	*434 / 3.05*	*431 / 3.22*	*429 / 2.80*	*428 / 4.02*	*427 / 2.71*	*425 / 2.55*
11	*400 / 2.37*	*398 / 2.59*	*396 / 2.96*	*394 / 3.44*	*393 / 2.89*	*391 / 3.36*
12	*324 / 3.29*	*323 / 2.16*	*321 / 2.92*	*319 / 3.20*	*319 / 2.23*	*317 / 2.86*
13	294 / 1.31	290 / 1.10	288 / 0.79	285 / 0.98	283 / 0.71	274 / 1.26
14	267 / 0.21	266 / 0.61				
15	239 / 3.54	239 / 4.49	237 / 1.94	236 / 3.24	235 / 3.36	234 / 4.22
16	192 / 3.20	199 / 1.21	195 / 3.81	197 / 1.81	197 / 1.52	196 / 2.80
17	176 / 2.54	184 / 3.09	179 / 2.94	172 / 2.10	170 / 1.47	165 / 3.39
18	167 / 1.35		165 / 1.30		158 / 0.65	
19	*142 / 3.40*	*140 / 4.69*	*139 / 0.98*	*137 / 2.51*	*136 / 1.95*	*136 / 1.67*

**Bands which fit the ionic radius relationship with a $R^2 > 0.90$ are shown in italics

Figure 1

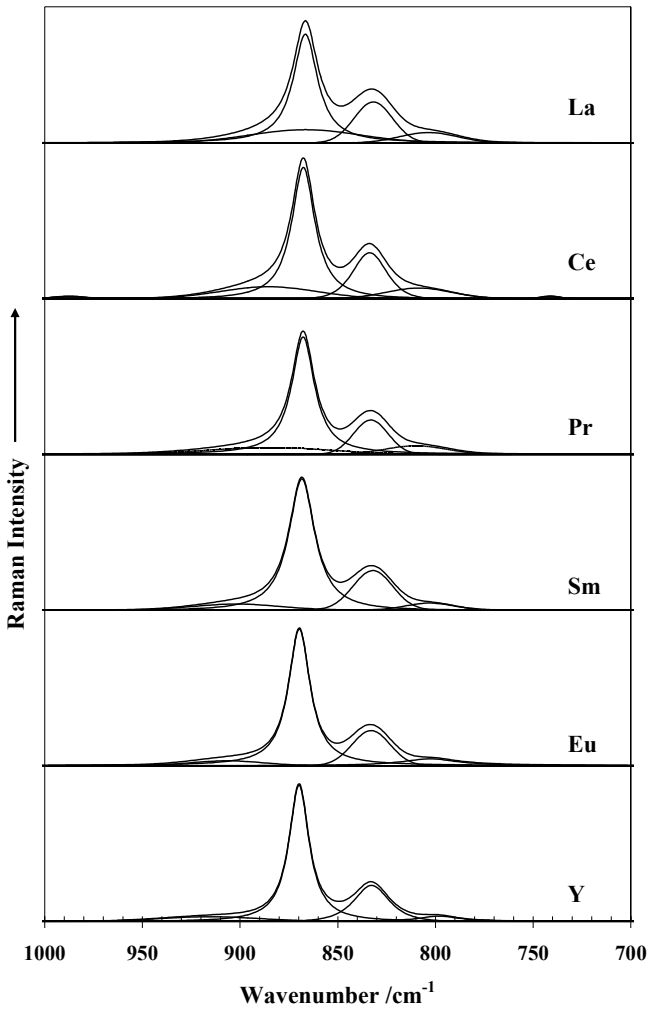
La
Ce
Pr
Sm
Eu
Y
Raman Intensity
1000
950
900
850
800
750
700
Wavenumber /cm-1

Figure 2

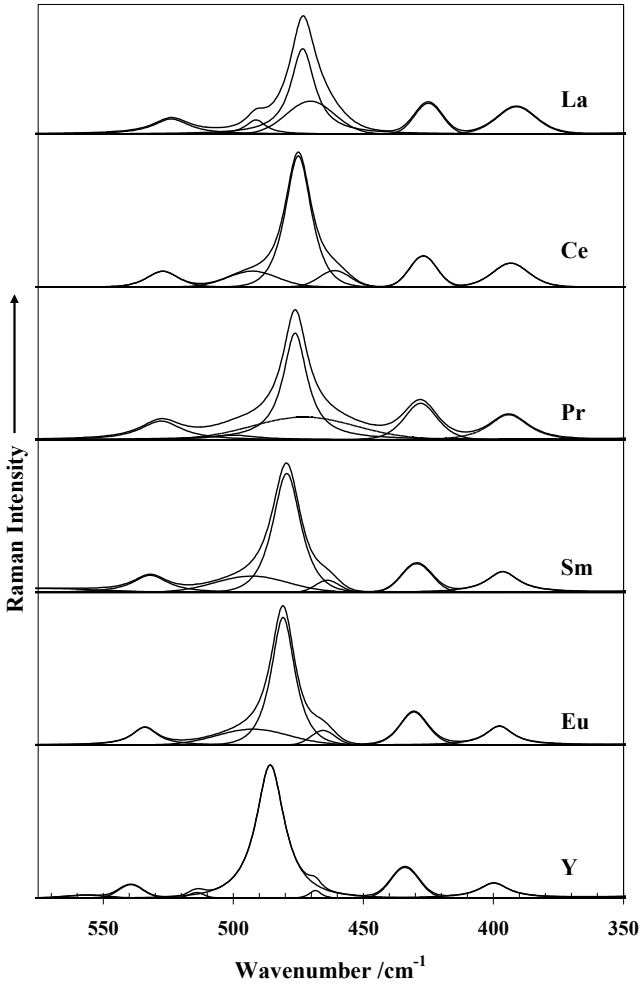
La
Ce
Pr
Sm
Eu
Y
Raman Intensity
550
500
450
400
350
Wavenumber /cm-1

Figure 3

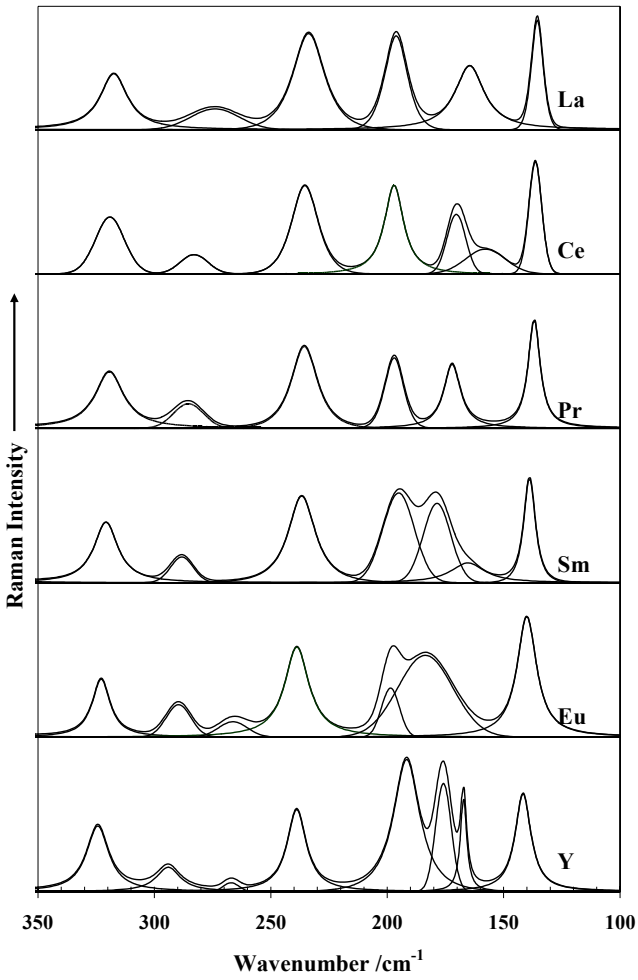
La
Ce
Pr
Sm
Eu
Y
Raman Intensity
350
300
250
200
150
100
Wavenumber /cm-1

Figure 4

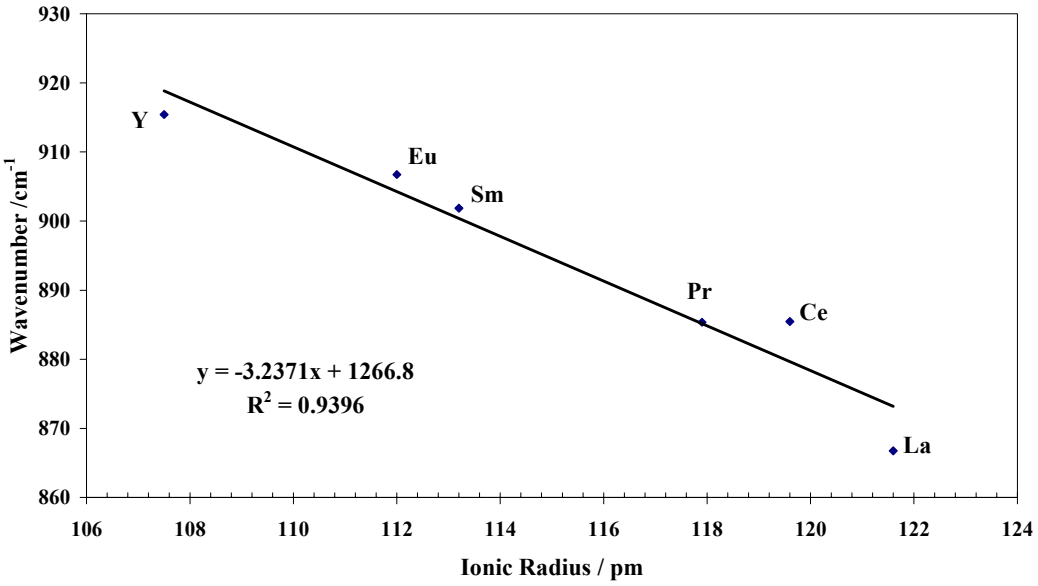
930
920
910
900
890
880
870
860
Wavenumber /cm-1
106
108
110
112
114
116
118
120
122
124
Ionic Radius / pm
Y
Eu
Sm
Pr
Ce
La
y = -3.2371x + 1266.8
R2 = 0.9396

Figure 5

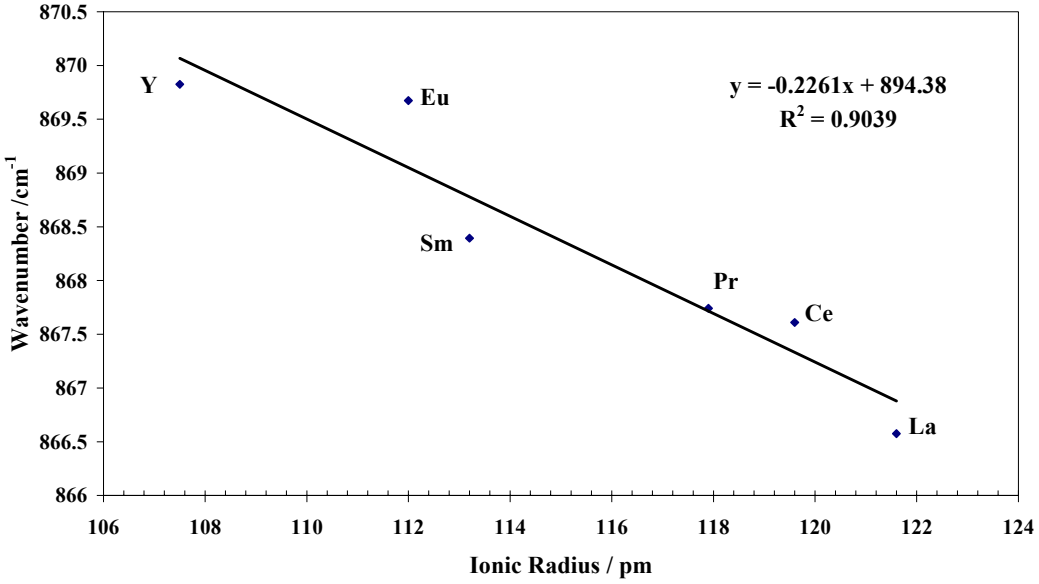
870.5
870
869.5
869
868.5
868
867.5
867
866.5
866
Wavenumber /cm-1
106
108
110
112
114
116
118
120
122
124
Ionic Radius / pm
Y
Eu
Sm
Pr
Ce
La
y = -0.2261x + 894.38
R2 = 0.9039

Figure 6

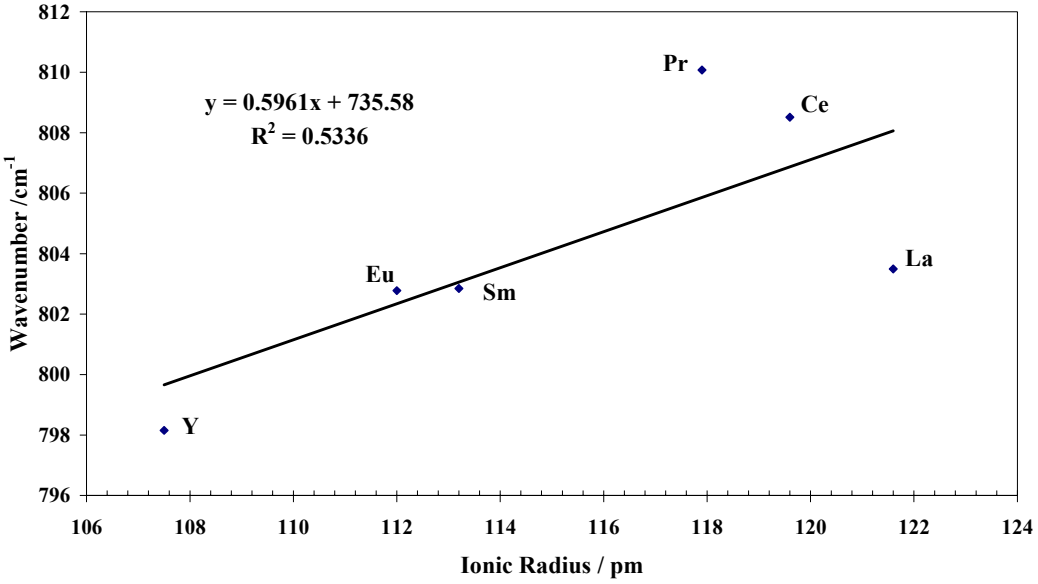
812
810
808
806
804
802
800
798
796
Wavenumber /cm-1
y = 0.5961x + 735.58
R2 = 0.5336
Pr
Ce
La
Eu
Sm
Y
106
108
110
112
114
116
118
120
122
124
Ionic Radius / pm

Figure 7

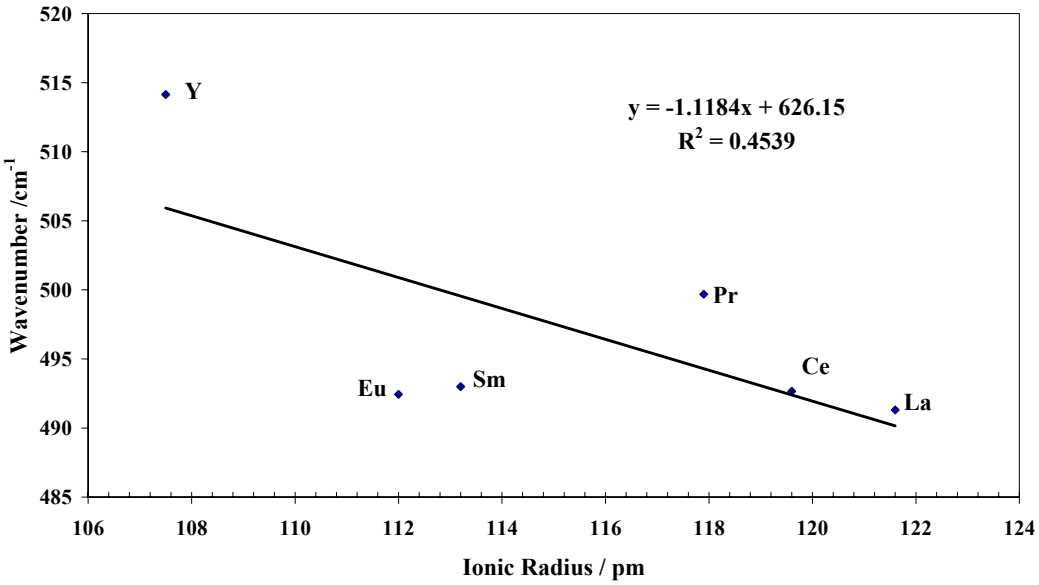
y = -1.1184x + 626.15
R2 = 0.4539
Y
Pr
Ce
La
Sm
Eu
Wavenumber /cm-1
Ionic Radius / pm
520
515
510
505
500
495
490
485
106
108
110
112
114
116
118
120
122
124

Figure 8

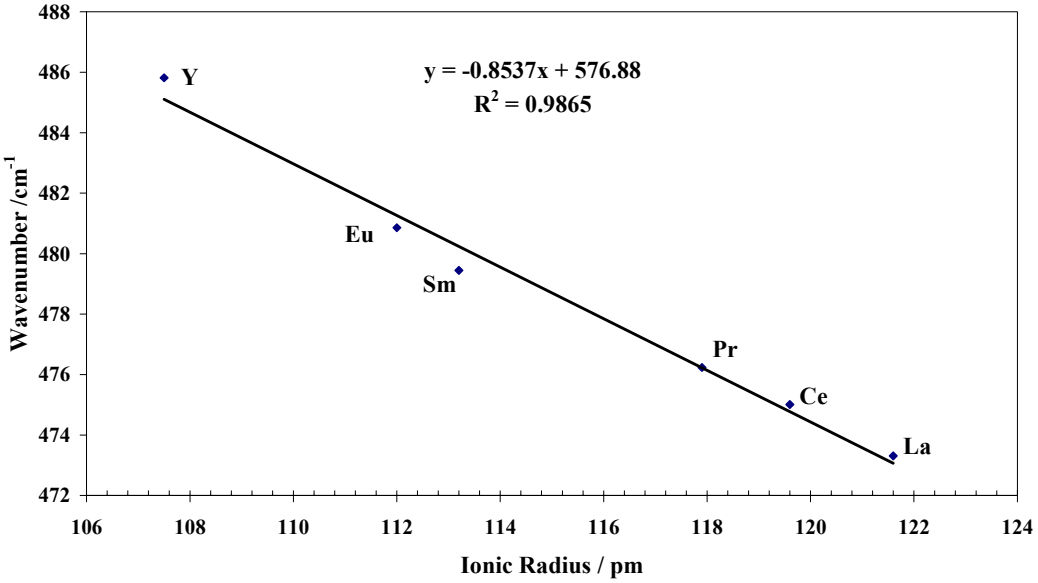
y = -0.8537x + 576.88
R2 = 0.9865
Y
Eu
Sm
Pr
Ce
La
Wavenumber /cm-1
Ionic Radius / pm
488
486
484
482
480
478
476
474
472
106
108
110
112
114
116
118
120
122
124

Figure 9

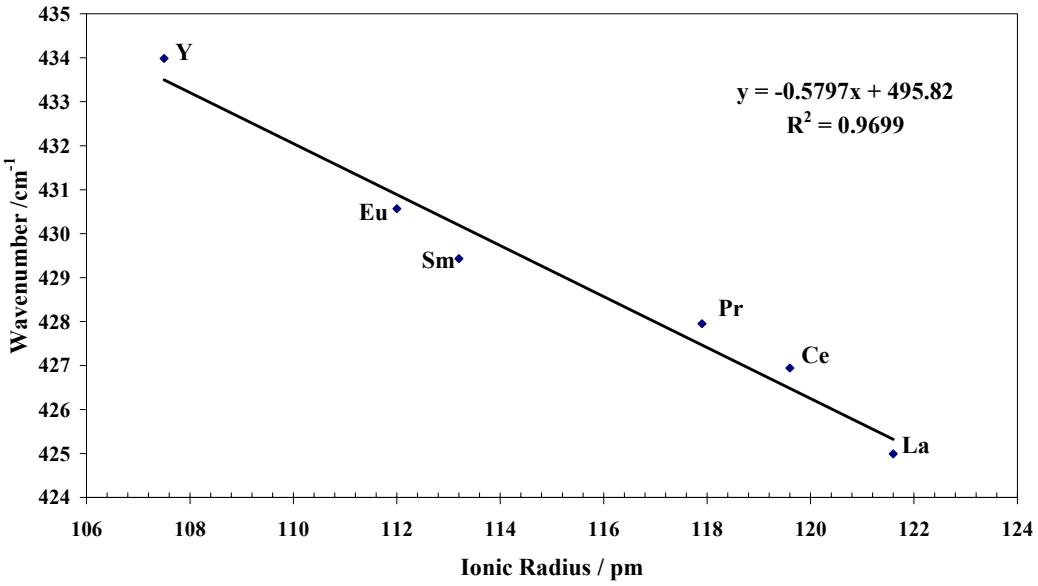
y = -0.5797x + 495.82
R2 = 0.9699
Y
Eu
Sm
Pr
Ce
La
Wavenumber /cm-1
Ionic Radius / pm
435
434
433
432
431
430
429
428
427
426
425
424
106
108
110
112
114
116
118
120
122
124

Figure 10

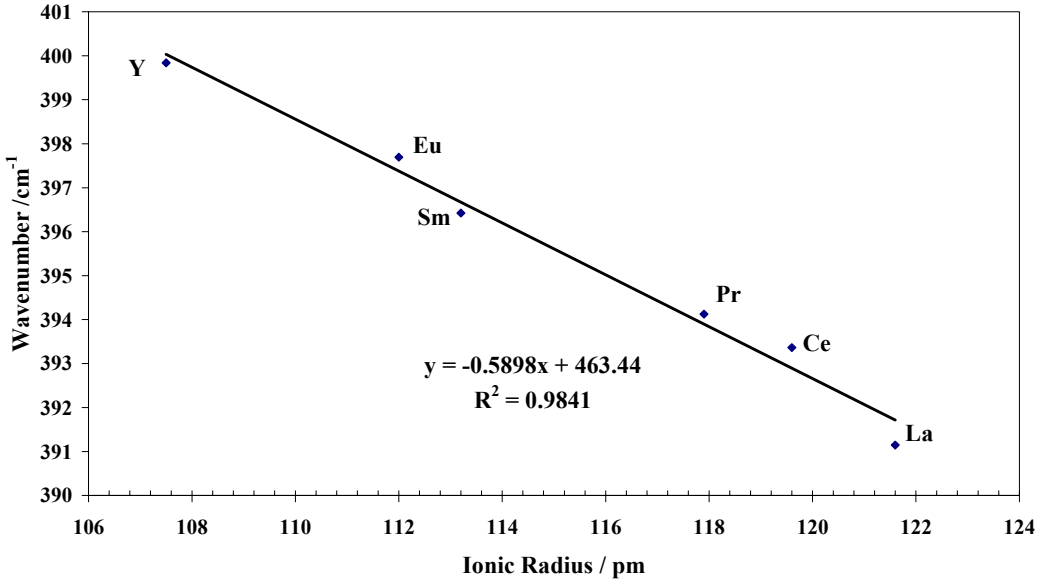
Wavenumber /cm-1
Ionic Radius / pm
Y
Eu
Sm
Pr
Ce
La
y = -0.5898x + 463.44
R2 = 0.9841
401
400
399
398
397
396
395
394
393
392
391
390
106
108
110
112
114
116
118
120
122
124

Figure 11

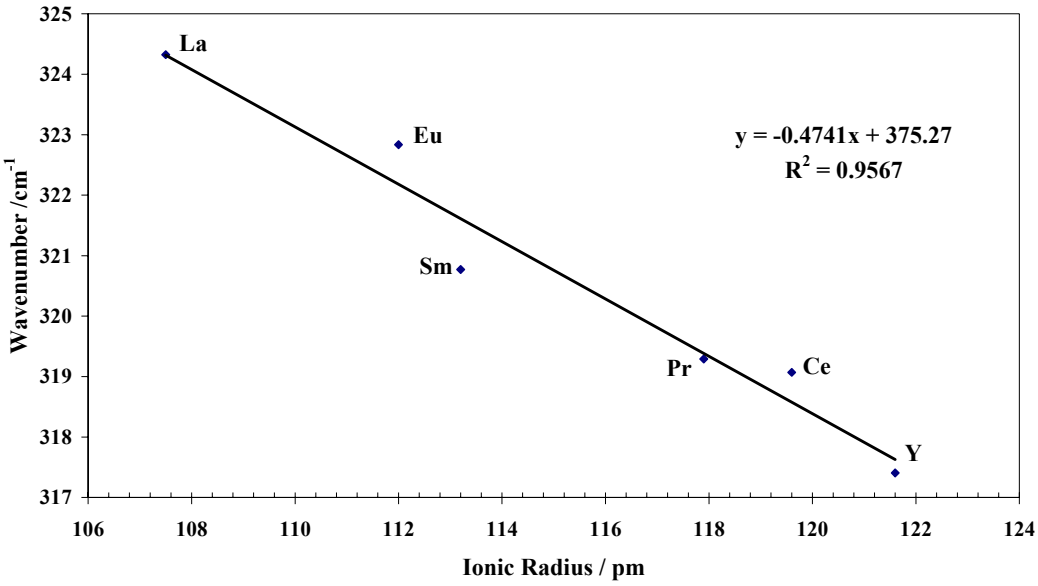
La
Eu
Sm
Pr
Ce
Y
y = -0.4741x + 375.27
R2 = 0.9567
Wavenumber /cm-1
Ionic Radius / pm
325
324
323
322
321
320
319
318
317
106
108
110
112
114
116
118
120
122
124

Figure 12

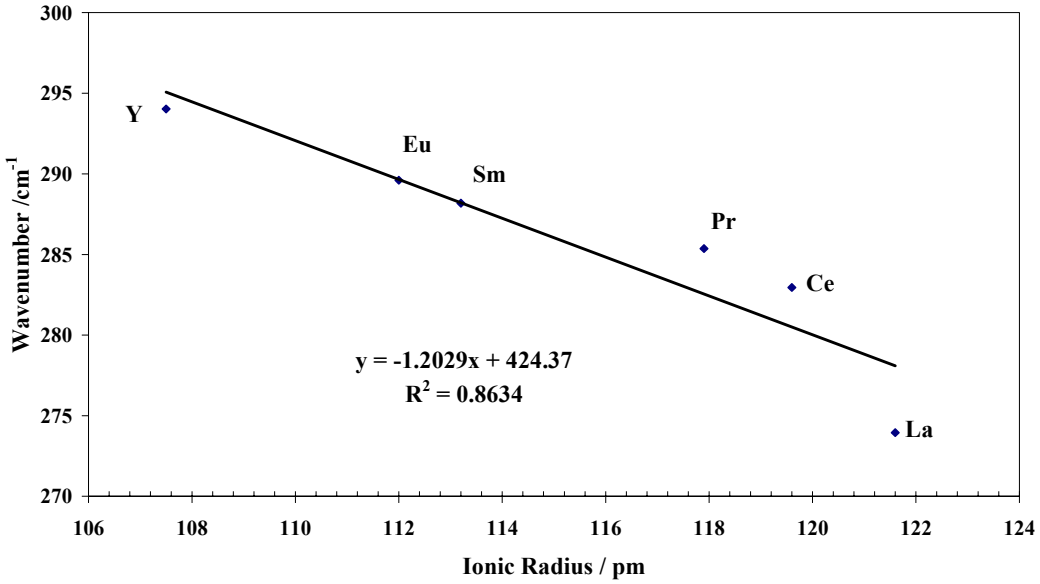

Figure 13

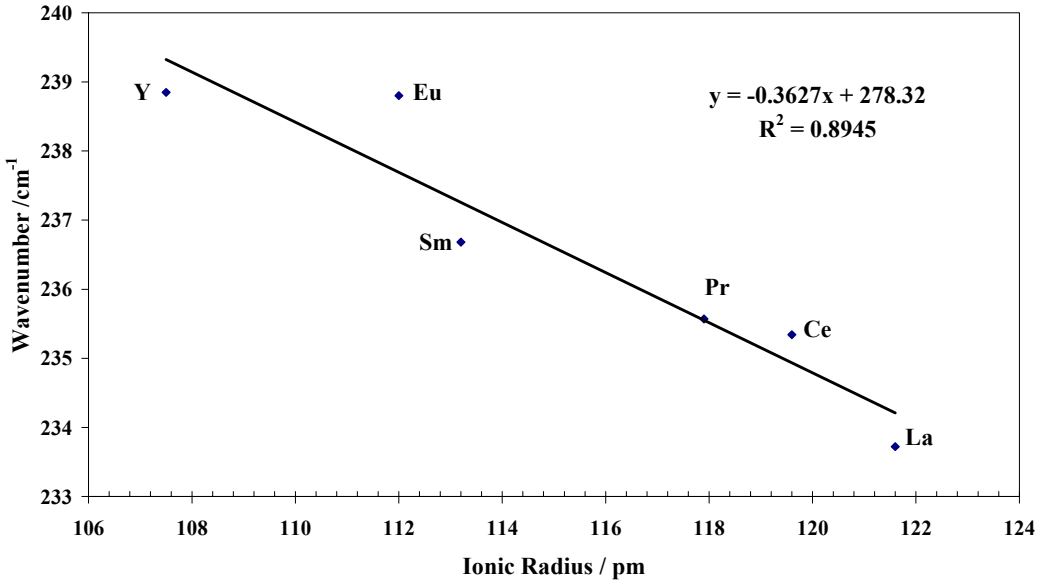

Figure 14

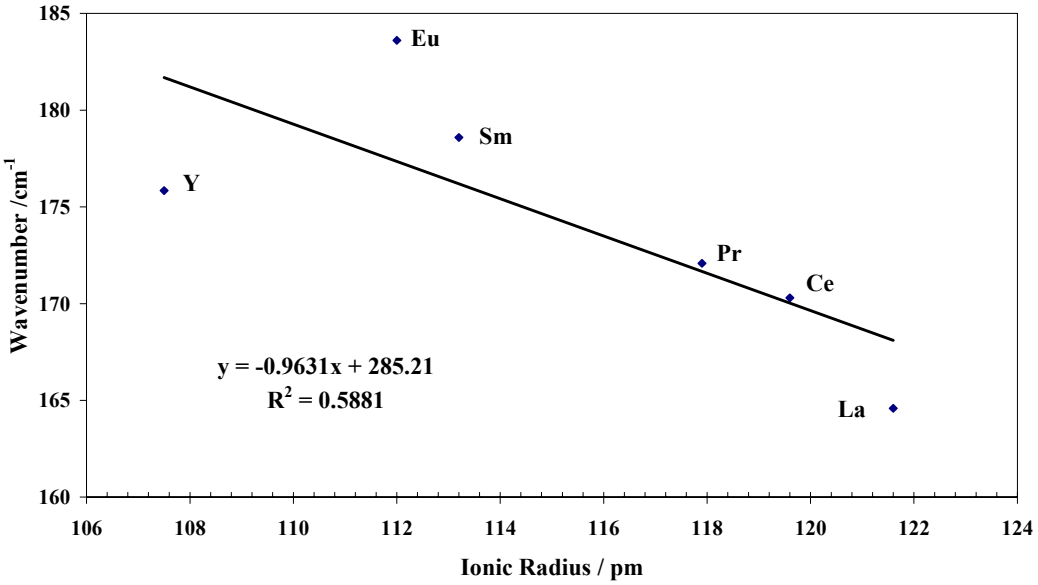

Figure 15